Proc. Nat. Acad. Sci. USA
Vol. 71, No. 1, pp. 1–5, January 1974

Scanning Transmission Electron Microscopy at High Resolution

(atom motion/electron optics/single atom visibility/carbon films/field emission source)

J. WALL, J. LANGMORE, M. ISAACSON, AND A. V. CREWE*

Enrico Fermi Institute, The University of Chicago, Chicago, Illinois 60637

Contributed by A. V. Crewe, September 6, 1973

ABSTRACT **We have shown that a scanning transmission electron microscope with a high brightness field emission source is capable of obtaining better than 3 Å resolution using 30 to 40 keV electrons. Elastic dark field images of single atoms of uranium and mercury are shown which demonstrate this fact as determined by a modified Rayleigh criterion. Point-to-point micrograph resolution between 2.5 and 3.0 Å is found in dark field images of micro-crystallites of uranium and thorium compounds. Furthermore, adequate contrast is available to observe single atoms as light as silver.**

The ability to obtain high resolution images of very small objects is of considerable importance in the biological and material sciences. The only instrument heretofore available for this purpose has been the conventional transmission electron microscope (CTEM).

Invented in the 1930's, the basic design of this instrument is an electron analog of the light microscope. The performance of the CTEM has steadily improved during the last few decades, and it is now limited primarily by diffraction effects and the large aberrations inherent in electromagnetic lenses.

For the moment, we will ignore the effects of chromatic aberration. This is justifiable if the electron energy is high enough. Then one can minimize the combined effect of diffraction and spherical aberration to calculate the objective aperture which gives the best instrumental resolution. In this case, a hypothetical point source of scattered electrons in the specimen plane would be imaged as a modified Airy disc whose radius to the first intensity minimum is given by

$$\delta = 0.43\ C_s^{1/4}\lambda^{3/4} \qquad [1]$$

where C_s is the coefficient of spherical aberration (generally of the order of 1 mm in high quality objective lenses) and λ is the wavelength of the incident electron (0.037 Å for 100-keV electrons) (1). The image of two incoherent point objects separated by this distance δ will have an intensity minimum between them of 0.75 of the peak intensity and will be resolved according to the modified Rayleigh criterion of Scherzer (1). In order to obtain this resolution, the objective aperture should subtend a half-angle at the specimen given by (2)

$$\alpha_{opt} = (4\lambda/C_s)^{1/4}. \qquad [2]$$

When operated in this fashion, most modern CTEMs are capable of achieving instrumental resolutions of 2–3 Å.

Abbreviations: STEM, scanning transmission electron microscope; CTEM, conventional transmission electron microscope; FWHM, full width at half maximum.

* Request reprints from A. V. Crewe.

This instrumental resolution is a property of the microscope itself and should not be confused with the specimen resolution which can be defined as the smallest resolved center-to-center distance between two objects on a micrograph and depends to a large extent upon image contrast. Instrumental resolution can, however, be measured from the images of nearly ideal point scattering objects. Single heavy atoms are suitable for this purpose because they are small compared to present instrumental resolutions and can give an elastic scattering dark field image with adequate contrast to be directly observed (3–6).

An electron microscope operating on a scanning principle was invented in 1938 by Von Ardenne (7). The scanning microscope operates by focusing the electron beam into a probe which is scanned across the specimen, while a detected signal resulting from electron interaction with the specimen is used to modulate the intensity on a synchronously scanned display tube. It has become widely used in the secondary emission mode, whereby slow secondary electrons ejected from the surface of thick specimens are detected (8). The resolution limit of these secondary emission microscopes is, however, determined not by the lenses used, but by the electron sources, which are generally hot tungsten filaments, of insufficient inherent brightness to provide adequate current in a diffraction limited spot.

Using a field emission electron source of high brightness, our laboratory has developed a practical scanning transmission electron microscope (STEM) (9, 10) which is limited by the electron lenses to the same ultimate resolution as the CTEM and which can form high contrast images with good signal to noise ratios. The fact that the CTEM and STEM have nearly the same ultimate resolution can be seen from the reciprocity theorem (11) which states that the path of rays through any optical system remains unchanged if the direction of rays is reversed. Therefore a STEM and a CTEM using equivalent operating conditions will produce images with the same resolution.

The purpose of this article is to demonstrate that an instrumental resolution of less than 3 Å has been attained by a STEM using a tungsten field emission source. The resolution has been measured in an unambiguous fashion by the observation of atoms of uranium and thorium spaced less than 3.4 Å apart and by measurement of the full width at half maximum of the spot profile as the beam is scanned across single mercury atoms.

MATERIALS AND METHODS

The Microscope. The optical system of the STEM used in this paper employs a tungsten field emission source and a

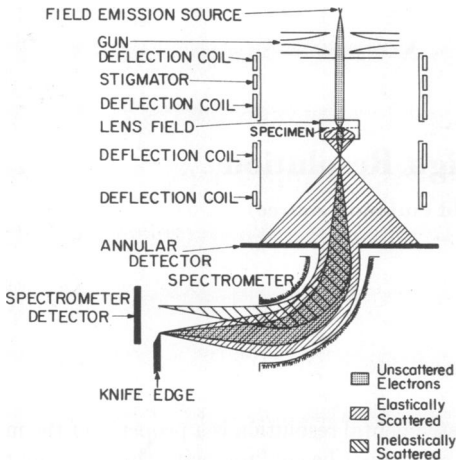

FIG. 1. Schematic diagram of the scanning transmission electron microscope (STEM) used in this paper. The ray envelopes are indicated showing the separation of the unscattered, elastically, and inelastically scattered electrons.

Butler-type electron gun (12) which is mounted directly on a short focal length magnetic lens (9). The gun is operated to produce electrons with an energy of 30–45 keV and the field emission source is located 1 cm above the first electrode. The source is generally operated at -4 keV with respect to the first electrode with typical values of field emission current being about 10 μA. The beam is accelerated between the first and second electrodes (the second electrode being at ground potential), passes through a 30-μm diameter aperture in the second electrode, and leaves the gun with a divergence half angle of 3.1×10^{-5} radians. The center of the objective lens field is 8 cm below the exit of the gun, and a magnetic double-deflection system and stigmator are located betweeen the gun and lens field (see Fig. 1). The lens has pole bore diameters of 3 mm and a pole gap of 3 mm, and is operated with the specimen located slightly above the center of the lens field. The focal length of the lens is $f = 1.15$ mm with a spherical aberration coefficient of $C_s = 0.46$ mm and a chromatic aberration coefficient of $C_c = 0.8$ mm. At 40 keV accelerating voltage, the probe radius can be defined by Eq. **1** and is $\delta = 2.5$ Å when only diffraction and spherical aberration of the objective lens are considered.

This value of δ is not the only contribution to the instrumental resolution since the effect of a finite source size must be taken into account for a scanning microscope. One can show that the effective source radius at the tip is approximately given by $r_0 \cong r_{tip} \sqrt{V_{tip}/V_1}$ where r_{tip} is the physical tip radius, V_{tip} is the energy spread of electrons leaving the source ($V_{tip} \cong 0.25$ eV for tungsten) and V_1 is the voltage between the tip and the first electrode (12).

Using $V_1 = 4$ keV and $r_{tip} \cong 750$ Å, we get $r_0 \cong 5$ Å. This effective source size at the tip is magnified by a factor of $M = 1/33$ by the gun and the objective lens, giving a Gaussian image of the source at the specimen plane of 0.18 Å radius. The radii of the chromatic aberration discs at the specimen plane due to the gun and magnetic lens are 0.18 Å and 0.4 Å, respectively, and the contribution of the spherical aberration of the gun to the probe size is almost two orders of magnitude less than that of the magnetic lens. While we have not yet performed accurate wave-optical calculations of these additional contributions to the probe size, it is clear that they should be small. Naively combining the effects in quadrature would give us an instrumental resolution of about 2.6 Å. In any case, we should expect a probe radius (peak to first minimum) of less than 3 Å.

The stabilities of the lens and high voltage supplies of the microscope are kept below 3 ppm and 10 ppm, respectively, which is adequate for such a resolution. The noise and drift of the deflection scans are kept below an equivalent 0.5 Å on the specimen.

In order to insure stable field emission, the microscope operates at about 10^{-10} Torr. This provides the additional advantage of a high vacuum around the specimen so that there is a negligible amount of contamination. No contamination can be observed during hundreds of repeated scans over areas as small as 200 Å on a side, even though the specimen is at room temperature and there are no anticontamination devices.

The optical design of the microscope is indicated schematically in Fig. 1. The electron beam is focused on the specimen by the first half of the magnetic lens and then brought to a second focus about 1 cm below the lens by the action of the lower half of the lens field. The angular demagnification produced by the lower half of the lens field allows for convenient collection of electrons scattered by the specimen.

A silicon surface barrier detector with a 200-μm diameter center hole (subtending a hollow cone from 0.02 radians to 0.2 radians at the specimen) is located below the magnetic lens. Unscattered electrons pass through the hole while 60–80% of the elastically scattered electrons strike this annular detector (13). About 90% of the inelastically scattered electrons also pass through this hole where they are separated from the unscattered electrons by a spherical electrostatic analyzer and detected by another silicon surface barrier detector (9, 10). A second set of magnetic double deflection coils is located below the specimen to "unscan" the unscattered beam, placing it on the optic axis at the annular detector plane.

The detector signals produced as the beam is scanned across the specimen are proportional to the scattered currents, and can be normalized using the beam current incident upon the specimen, converted to digital form, and stored on magnetic tape. Measurements can then be performed directly on the recorded signal and information displayed on a TV display system (14) or photographed on a high resolution cathode ray tube. Since we can obtain over 10^{-10} amps in the focused spot, we record a 512×512 line picture in 8.5 sec with adequate signal to noise in the image.

Specimen Preparation. Careful preparation of the carbon substrates used to support the specimens was of utmost importance since heavy atom contaminants on the carbon films may be confused with the actual single atom specimens (15). Electron beam vacuum evaporation of high purity graphite (National AGKSP) onto cleaved mica or NaCl was performed in an oil-free, ion-pumped bell jar. The pressure before evaporation was always maintained between 10^{-7} and 10^{-9} Torr. Evaporation times between 10 and 100 sec were used.

The carbon films were floated off their substrates onto the surface of deionized water (Millipore Super Q). They were then picked up on 100-mesh gold grids which had previously been covered by a holey collodion film and carbon coated. The resultant films were between 10 and 30 Å thick as determined by their elastic scattering cross-sections, assuming a film density of 2 g/cm^3. These films were hydrophilic and had a heavy atom

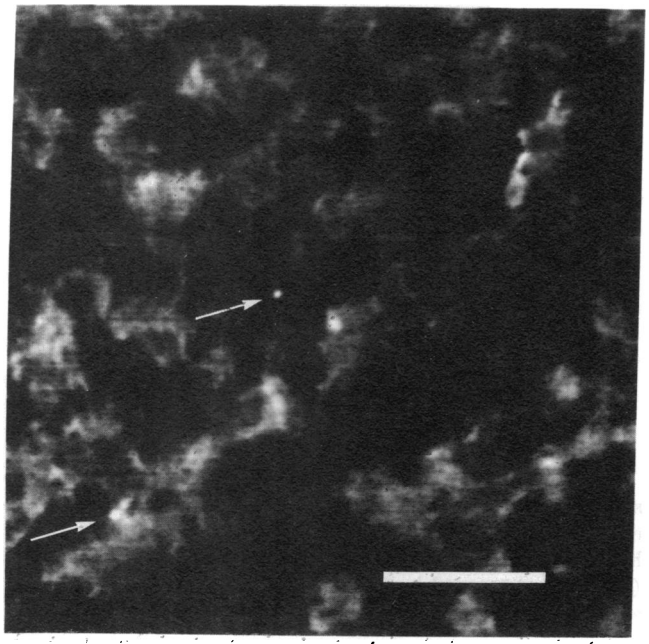

FIG. 2. A representative micrograph of a carbon film before application of the heavy atom specimen. The scale bar represents 50 Å.

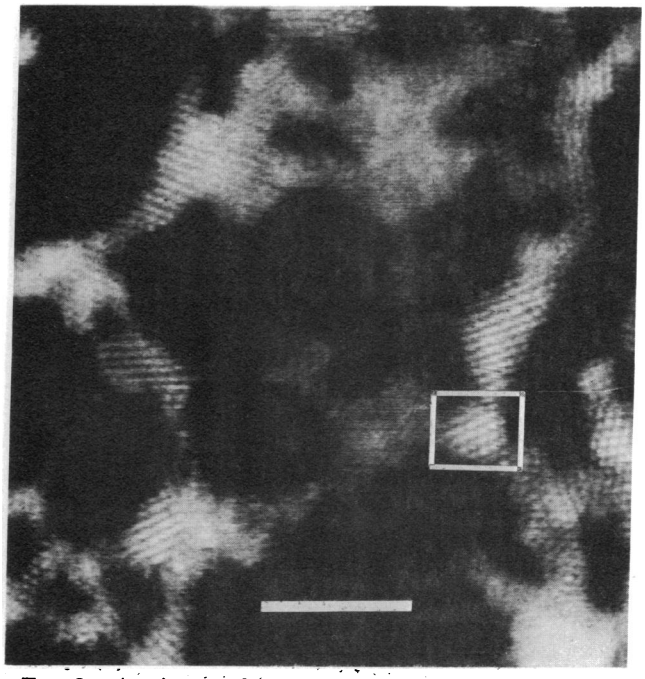

FIG. 3. A micrograph of a thorium specimen at 33.5 keV showing several micro-crystallites. The scale bar indicates 50 Å. Point-to-point separations within the rectangle vary from 2.8 to 3.4 Å.

contamination density of about 1 heavy atom per 10^4 Å^2 of film area.

Thorium specimens were prepared by mixing equal volumes of 10^{-3} M $Th(NO_3)_4$ (Alfa ultrapure) and 10^{-3} M NaOH (Baker Analyzed). This solution was then diluted 10-fold after 30 min. About 5 μl of this solution was placed on a carbon film. After 1 min it was then blotted off from one edge of the grid with filter paper.

Uranium specimens were prepared by titrating a 10^{-4} M solution of $UO_2Cl_2{:}3H_2O$ (Alfa) to pH 3 with HCl (Baker Analyzed). The final solution was placed on a carbon film in the same manner as with the thorium solution.

Single atom mercury and silver specimens were prepared by allowing 5 μl of freshly made 10^{-4} M aqueous solution of mercuric acetate (Baker Analyzed) or silver acetate (Allied Chemical) to remain on the carbon film coated grid for 15 sec before drawing it off with a polypropylene pipet. Each carbon film was examined carefully at high resolution immediately before preparing the specimen, to insure that fewer than 0.5 extraneous heavy atoms per 10^4 Å^2 were present.

Micrographs. The magnification of all micrographs was calibrated to 5% accuracy by measuring a diffraction grating replica at a field of view of 6 μm. The magnification for any other field of view was determined by the ratio of the scanning coil current at that field of view to the scanning current for the 6 μm field of view. A slight distortion occurs in the scans due to a 0.02 G stray ac magnetic field in our laboratory. This amounts to a 5% nonlinearity for a 200-Å field of view.

All micrographs shown in this paper were obtained using the scattered electron current detected with the annular detector below the lens (see Fig. 1). The signal output from this detector is nearly proportional to the elastic scattering intensity and will be referred to as the elastic signal. Since elastic scattering increases approximately as $Z^{3/2}$, where Z is the atomic number of the material (13), this annular detector signal is a strong function of the atomic number. For example, a single thorium or uranium atom is expected to produce as many elastically scattered electrons as about 60 carbon atoms, and thus should be easily detectable on a sufficiently thin carbon film.

In order to obtain a maximum signal to noise ratio in the micrographs and demonstrate the instrumental resolution, the micrographs shown were taken with incident electron doses per micrograph of 10^4–10^5 electrons/Å^2. This is about two orders of magnitude greater than the minimum dose required for visibility (16).

RESULTS

An elastic dark field micrograph of a typical carbon film substrate, which had been evaporated onto NaCl, is shown in Fig. 2 before the application of a heavy atom solution. The micrograph was obtained with suitable amplification and dc level suppression to best show the carbon film structure. Note that there are only two objects on this 4×10^4 Å^2 area which have the elastic scattering intensity, the size, and the shape of single heavy atoms. Similar spot densities were found after application of a "specimen" consisting only of water.

Fig. 3 shows a representative elastic dark field micrograph of a thorium specimen. Note the existence of microcrystals and lattice planes in many directions and in some cases two-dimensional hexagonal nets. Optical diffraction from these crystallite nets and from similar micrographs indicate that the crystallites are, in fact, hexagonal, but not quite regular with average spacing of 3.3 ± 0.2 Å. We can see directly from Fig. 3 that the lattice spacings vary from 2.5 to 3.6 Å. In the regions where the crystallites are seen as two-dimensional nets of atoms one can resolve point-to-point separations less than 3.0 Å. The exact composition of these crystals is not known; however, from the lattice spacings and the hexagonal structure measured on the micrographs, they might be composed of ThO_2 or ThC_2.

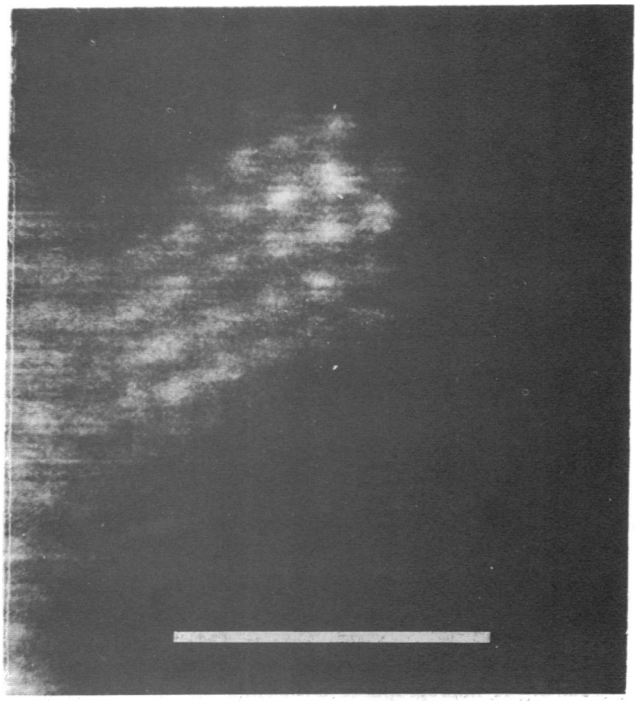

FIG. 4. Micrograph of a typical micro-crystallite seen on uranium specimens, taken at 33.5 keV. The scale bar indicates 20 Å. Point-to-point spacing in this crystallite varies between 2.5 and 3.6 Å.

A point-to-point specimen resolution of 3 Å or less can also be demonstrated on uranyl chloride specimens. In Fig. 4 we show a typical example of a microcrystal with a hexagonal-like lattice. The bar represents 20 Å. Note again that the lattice is imperfect with point-to-point atom spacings varying between 2.5 and 3.6 Å. Optical diffraction from a micrograph of this crystallite reveals that the average spacing is 3.3 ± 0.2 Å. Note also that the spacings between rows of atoms looking in the direction of the rows averages 2.9 ± 0.2 Å.

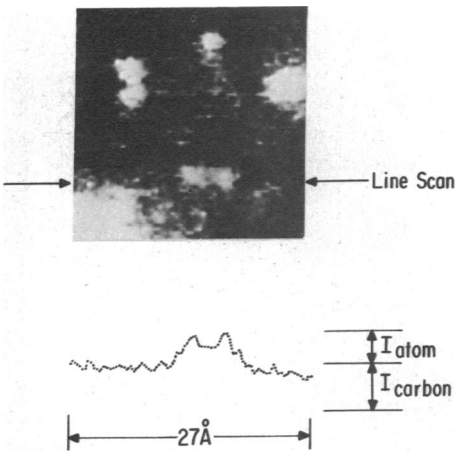

FIG. 6. A highly magnified region of a typical uranium specimen. The intensity distribution along the horizontal line indicated by arrows beside the micrograph is presented in the lower half of the figure. The dip midway between the single atom peaks (which are separated by 3.4 Å) is 0.65 of the single atom peak signal.

It should be pointed out that the thorium specimens generally tend to form only micro-crystallites, whereas the uranyl specimens form either crystallites (see Fig. 4) or chains. A typical micrograph of uranium chains is shown in Fig. 5. The

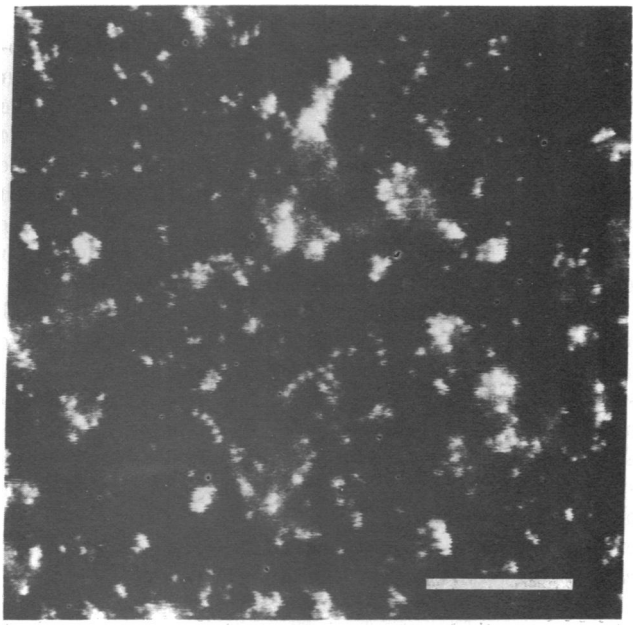

FIG. 5. Micrograph of a uranium specimen showing single atom chains, at 33.5 keV. The scale bar indicates 50 Å. Point-to-point separation of atoms in the chains varies from 2.8 to 3.9 Å.

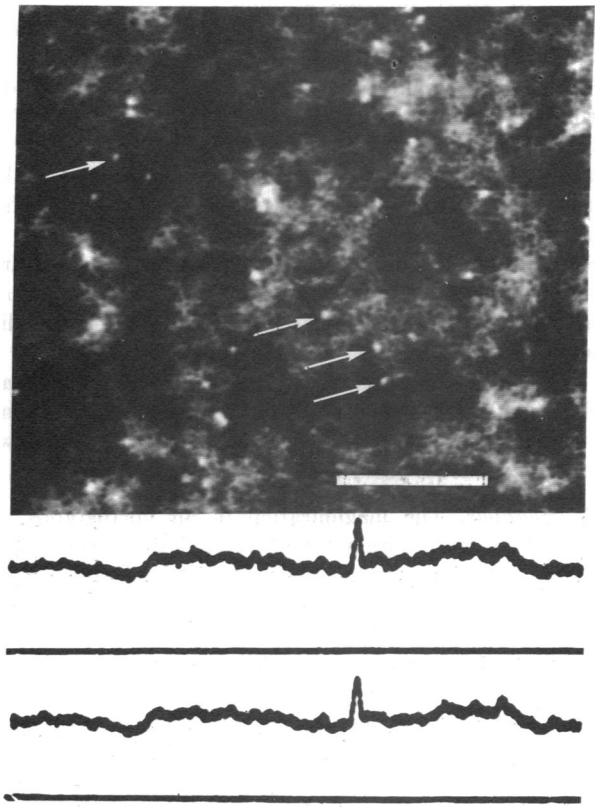

FIG. 7. A representative area on a mercuric acetate specimen at 42.5 keV. A few of the single atoms are indicated by arrows. The scale bar indicates 50 Å. Two different line scans over the same atom on this specimen are shown beneath the micrograph. The scale of the line scans and the micrograph are equal. The FWHM of the mercury spot is 2.5 ± 0.2 Å.

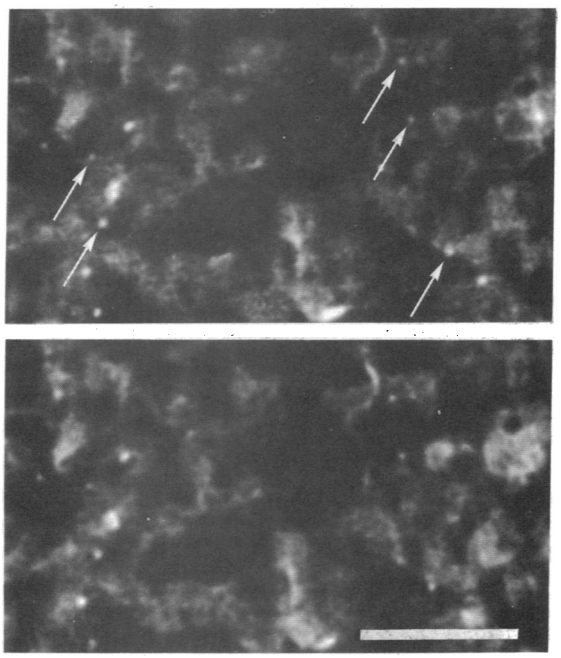

FIG. 8. The first (*upper*) and tenth (*lower*) exposures of the same area of a silver acetate specimen. The scale bar represents 50 Å.

point-to-point separation between atoms in the chains is in many cases about 3 Å or less.

One can obtain a more quantitative estimate of instrumental resolution from a line scan across one or two atoms. This is performed easily in the STEM since the signals from the microscope are proportional to the scattered electron intensity. In Fig. 6 we present a highly magnified portion of a uranium specimen. The image was obtained from the elastically scattered signal using 33.5 keV electrons and stored directly on magnetic tape. The micrograph shown was taken from the magnetic tape replay. Below the micrograph we show the plot of elastic scattered intensity versus spatial position along a line shown in the micrograph by arrows. The separation of the peaks due to the two atoms in that line scan is 3.4 ± 0.1 Å. The intensity dip between the two atom peaks is about 65% of the peak height. Since two point objects placed one resolution distance, δ, apart are expected to dip to 75% between them if the resolution conditions are given by Eqs. **1** and **2**, the instrumental resolution is better than 3.4 Å.

The full width at half maximum (FWHM) of the probe distribution obtained using the aperture condition of Eq. **2** is nearly equal to the radius from the peak to first minimum given by Eq. **1**. Therefore, the FWHM of the intensity profile obtained by scanning the probe across a nearly ideal point object (a single heavy atom) is almost equal to the resolution distance, δ, given in Eq. **1**. In Fig. 7 we show an elastic dark field micrograph of single mercury atoms on a thin carbon film and two different elastic intensity profiles obtained by scanning the beam across a particular atom and displaying the annular detector signal. The FWHM of the peaks in these line profiles is 2.5 ± 0.2 Å. In the time between the first and second recorded scan, 10^7 electrons/Å^2 were incident upon the mercury atom.

The use of this single atom visibility to localize chemical sites in biological molecules may be restricted by heavy atom motion in the beam. Thorium and silver atoms, for instance, are more stable than are mercury and uranium. Fig. 8 shows a portion of a silver acetate specimen on the first and tenth scan at 43 keV. The single silver atoms (arrows) did not move during a time of 80 sec and an exposure to 5×10^5 electrons/Å^2. Notice also that the structure of the carbon substrate has not significantly changed during the irradiation.

DISCUSSION

We have shown that it is possible to obtain better than 3 Å instrumental resolution with a STEM using 30 to 40 keV electrons and a high brightness electron source. Although the resolution obtainable with a STEM is the same as that obtained in a CTEM with the same objective lens, the ability of the STEM to simultaneously collect different types of scattered electrons (e.g., elastic, inelastic, and unscattered) allows one to obtain more information per scattering event than with the CTEM and therefore to minimize radiation damage (16). This is of considerable importance in biological electron microscopy.

Atoms as light as silver ($Z = 47$) can be directly visualized in a STEM using 43-keV electrons. Since the signal-to-noise available from a single heavy atom in a carbon matrix increases as the instrumental resolution improves, the increase in resolution attainable by using higher voltages (e.g., $\delta < 2$ Å at 100 keV) should allow sufficient signal-to-noise to be able to directly visualize single atoms over more than half the periodic table.

This work was performed under the auspices of the U.S. Atomic Energy Commission.

1. Scherzer, O. (1949) *J. Applied Physics* **20**, 20–29.
2. Haine, M. E. & Cosslett, V. E. (1961) in *The Electron Microscope: The Present State of the Art* (Spon Ltd., London), p. 56.
3. Crewe, A. V., Wall, J. & Langmore, J. (1970) *Science* **168**, 1338–1340.
4. Henkelman, R. M. & Ottensmeyer, F. P. (1971) *Proc. Nat. Acad. Sci. USA* **68**, 3000–3004.
5. Hashimoto, H., Kumao, A., Hino, K., Yotsumoto, H. & Ono, A. (1971) *Jap. J. Appl. Phys.* **10**, 1115–1116.
6. Wall, J., Langmore, J., Isaacson, M. & Crewe, A. V. (1973) *Proc. Thirty-First Annual EMSA Conference*, 230–231.
7. von Ardenne, M. (1938) *Z. Phys.* **109**, 553–572.
8. Smith, K. C. A. & Oatley, C. W. (1955) *Brit. J. Applied Physics* **6**, 391–399.
9. Crewe, A. V. & Wall, J. (1970) *J. Mol. Biol.* **48**, 375–393.
10. Crewe, A. V. (1970) *Quart. Rev. Biophys.* **3**, 137–179.
11. Crewe, A. V. & Wall, J. (1970) *Optik* **30**, 461–474.
12. Crewe, A. V., Eggenberger, D., Wall, J. & Welter, L. (1968) *Rev. Sci. Instrum.* **39**, 376–383.
13. Langmore, J. P., Wall, J. & Isaacson, M. (1973) *Optik* **38**, 335–350.
14. Beck, V. (1973) *Rev. Sci. Instrum.* **44**, 1064–1066.
15. Langmore, J., Wall, J., Isaacson, M. & Crewe, A. V. (1973) *Proc. Thirty-first Annual EMSA Conference*, 76–77.
16. Isaacson, M., Johnson, D. & Crewe, A. V. (1973) *Radiat. Res.* **55**, 205–224.